Research Article

Mitigated multipath interference in PAM4 IM/DD optical links using instantaneous mean intensity addressing

YIBIN LI, ¹ ZIXIAN WEI, ¹ D LIHANG LIU, ² H. Y. FU, ² D AND CHANGYUAN YU^{1,*} D

Abstract: Multipath interference (MPI) poses a significant challenge for 4-level pulse amplitude modulation (PAM4) signals in short-reach intensity modulation and direct detection (IM/DD) interconnect systems. MPI, arising from signal reflections due to the multiple fiber connectors, introduces irregular intensity fluctuations across PAM4 levels, severely degrading the system performance. This work proposes an MPI noise mitigation scheme, instantaneous mean intensity addressing (IMIA), which suppresses the MPI noise by utilizing an instantaneous mean intensity table and an MPI noise table for real-time noise extraction and removal. Simulation results in a 50-Gbps PAM4 transmission system under single and multiple forward-traveling reflected light (FTRL) scenarios demonstrate the effectiveness of the proposed IMIA scheme across varying MPI conditions. In both scenarios, the IMIA scheme achieves over 6 dB and over 4 dB MPI tolerance for the 7% hard-decision forward error correction (HD-FEC) and KP4-FEC criteria, respectively. Moreover, the integration of the IMIA scheme with a noise whitening filter (NWF) and maximum likelihood sequence estimation (MLSE) provides an additional 2 dB of MPI tolerance improvement.

© 2025 Optica Publishing Group under the terms of the Optica Open Access Publishing Agreement

1. Introduction

The rapid advancement of cloud computing, big data analysis, and artificial intelligence has led to an exponential growth in IP traffic, particularly within short-reach optical communication networks [1]. Short-reach optical links, covering distances below 40 km, serve as the backbone for interconnecting servers within and between data centers [2]. Intensity modulation and direct detection (IM/DD) scheme is widely adopted in data center environments due to their cost-effectiveness and power efficiency [3–5]. Among the various IM/DD modulation formats, 4-level pulse amplitude modulation (PAM4) has become the preferred choice, offering a balance between bandwidth efficiency and system complexity [6]. PAM4 has already been standardized for four-lane 400 Gigabit Ethernet (GbE) [7].

As data center networks expend, millions of interconnected optical links create increasingly complex link topologies [8]. A significant challenge in such environments is multipath interference (MPI) [9,10], caused by signal reflections at dirty fiber connectors. These reflections produce delayed replicas of the transmitted signal, which interfere with the original signal at the receiver. The multi-level *m*-PAM modulation in IM/DD systems is particularly susceptible to the effects of MPI [11], making MPI mitigation essential in the design and operation of data center networks.

Mitigating MPI in PAM4-based IM/DD systems has attracted considerable research interest, and various approaches have been proposed. One common method involves using a high-pass filter (HPF) at the receiver to mitigate low-frequency carrier-carrier beat noise caused by MPI [12]. However, for lasers with broader linewidth, the HPF requires a high cut-off frequency

#553239 Journal © 2025 https://doi.org/10.1364/OE.553239

Received 20 Dec 2024; revised 22 Jan 2025; accepted 27 Jan 2025; published 22 Apr 2025

¹Department of Electrical and Electronic Engineering, The Hong Kong Polytechnic University, Kowloon, Hong Kong 999077, China

²Tsinghua Shenzhen International Graduate School, Tsinghua University, Shenzhen 518055, China *changyuan.yu@polyu.edu.hk

to remove the MPI noise effectively which may also filter out essential low-frequency signal components, resulting in power penalties, resulting in additional power penalties. MPI-induced impairment on PAM4 signals often appears as irregular intensity fluctuations across the PAM levels. To address this, two specific algorithms, A1 and A2, have been integrated into the receiving digital signal processing (DSP) framework [13]. The first algorithm, A1, smooths the PAM4 signals by subtracting the mean value of the symbols received, while the second algorithm, A2, estimates the MPI noise and removes it from the received PAM4 signals. The cascade of the two algorithms effectively suppresses MPI noise. Although effective, these algorithms are computationally intensive, requiring hundreds or thousands of taps. Moreover, A2 relies on predecision PAM symbols and the optimization of multiple weighting factors, further complicating its implementation. Low-complexity alternatives, such as balanced coding schemes that reduce low-frequency components of PAM4 signals at the transmitter [14], have shown comparable performance to the combined A1 and A2 algorithms. Additionally, a DSP-based statistical technique has been developed to detect high MPI levels, enabling timely fiber maintenance to prevent signal degradation [15].

In our previous works, we proposed an adaptive decision threshold (ADT) scheme to effectively decode the MPI-impaired PAM4 signals [16]. Rather than directly mitigating noise, the ADT scheme dynamically updates decision thresholds based on real-time observations of the received signal. This approach allows the thresholds to adapt to fluctuations in MPI-impaired signals. However, because the ADT scheme directly decodes the PAM4 signal after processing, it is incompatible with additional processing algorithms, such as the noise whitening filter (NWF) and maximum-likelihood sequence estimator (MLSE) [17], which are typically used to mitigate the colored noise introduced by the feedforward equalizer (FFE).

In this paper, we propose a novel MPI noise mitigation scheme based on instantaneous mean intensity addressing (IMIA). Due to the irregular fluctuation, the MPI noise varies within PAM4 signal over time. By establishing an instantaneous mean intensity table and an MPI noise table, the IMIA scheme can dynamically extract MPI noise and allow real-time noise removal through reference to these tables. The proposed IMIA scheme is evaluated through simulations in a 50-Gbps PAM4 transmission system, considering both single and multiple reflected signal scenarios. The simulation results show that the proposed IMIA scheme has a comparable performance to the ADT scheme. Simulation results demonstrate that the IMIA scheme offers comparable performance to the ADT scheme. Additionally, the IMIA scheme does not directly decode the signal but instead focuses on extracting and removing MPI noise, enabling seamless integration with NWF and MLSE. This integration allows the IMIA scheme to achieve further performance improvements by addressing additional noise sources beyond MPI.

The rest of this paper is organized as follows. Section 2 explains the model of MPI noise. Section 3 introduces the principle of our proposed IMIA scheme for MPI noise mitigation. Section 4 describes the simulation setup for the evaluation of the proposed IMIA scheme. Section 5 presents the simulation results and discussion. Section 6 gives the conclusion of the paper.

2. MPI model

Multi-node reflection in short-reach scenarios can occur due to the high density of interconnections typically found in environments like data centers. These networks often involve numerous fiber connectors, where the air gap between two connector end faces creates refractive index discontinuities, causing part of the transmitted light to be reflected. This issue is further exacerbated when connectors are dirty. Each pair of reflective surfaces within the fiber link generates a forward-traveling reflected light (FTRL), as shown in Fig. 1. The FTRLs fall behind the original signals by several kilometers, resulting in delays that extend well beyond thousands of baud periods compared to the original transmission. As a result, traditional equalization schemes, which are typically used to compensate for intersymbol interference (ISI), are ineffective

against MPI. This is because the introduced delay exceeds the time span that equalizer taps can compensate for.

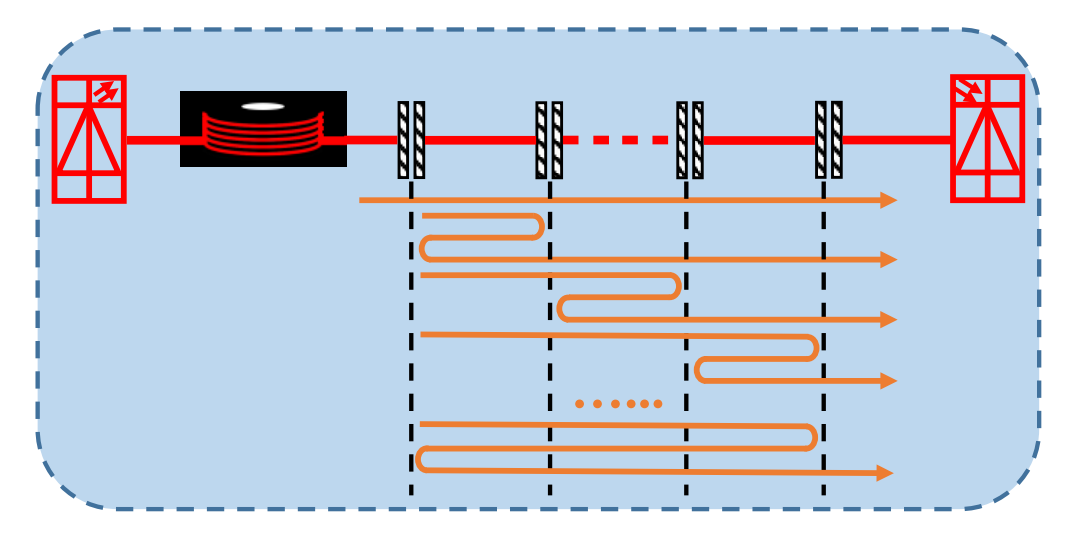


Fig. 1. Generation of MPI noise.

The optical field of the transmitted light is

$$E_0(t) = A(t)e^{j[\omega t + \varphi(t)]} \tag{1}$$

where A(t) represents the amplitude of the modulated signal, ω is the center frequency of laser and $\varphi(t)$ denotes the laser phase noise. Assuming that all reflective points within the fiber link exhibit the same return loss, denoted as R, the total optical field at the receiver, including the contributions from the FTRLs, is expressed as

$$E_{MPI}(t) = E_0(t) + \sum_{k=1}^{N} \sqrt{R^2} cos\alpha_k E_0(t - \tau_k)$$
 (2)

Here, N is the total number of FTRLs, α_k is the relative polarization angle and τ_k is the time delay associated with the kth FTRL. To simplify the analysis, we will focus on the case with a single FTRL, setting the polarization angle $\alpha_k = 0$ to maximize the impact of the MPI. With this assumption, the expression for the optical field simplifies to

$$E_{MPI}(t) = E_0(t) + RE_0(t - \tau) \tag{3}$$

At the receiver, after square-law detection, the received current can be written as

$$EI(t) = \eta |E_0(t)|^2 + 2\eta R \times Re[E_0^*(t)E_0(t-\tau)] + \eta R^2 |E_0(t-\tau)|^2$$
(4)

where η represents the responsivity of photodetector. Since return loss values in optical systems are typically low, the third term on the right-hand side can be reasonably neglected. Therefore, the expression for the received current simplifies to

$$I(t) \approx \eta |A(t)|^2 + 2\eta RA(t)A(t-\tau) \times \cos[\omega \tau + \phi(t, \tau)]$$
 (5)

Analyzing the interference term $2\eta RA(t)A(t-\tau) \times \cos[\omega\tau + \phi(t,\tau)]$, it is apparent that the MPI noise is amplitude dependent. Specifically, signals with larger amplitudes experience a more significant impact from MPI noise. This suggests that higher PAM levels are inherently more vulnerable to the adverse effects of MPI noise.

Additionally, the interference results in laser relative intensity noise (RIN). When the delay τ exceeds the laser coherence time, i.e., when $2\pi\Delta\nu\tau\gg 1$, RIN is approximately given by

$$RIN(f) \approx \frac{4R^2}{\pi} \left[\frac{\Delta v}{f^2 + \Delta v^2} \right]$$
 (6)

where Δv is the laser linewidth. This situation is particularly common in data center connections, where the fiber length spans several kilometers. The laser linewidth plays a crucial role in determining the impact of noise in IM/DD systems. Specifically, a broader laser linewidth amplifies the impact of MPI, leading to more severe interference in communication links.

3. Proposed MPI noise mitigation scheme based on IMIA

Figure 2(a) and Fig. 2(b) present the signal envelopes of PAM4 without and with the presence of MPI noise, respectively. It is evident from two figures that MPI noise introduces ripples on the received PAM4 signal envelope. The four PAM levels with the impact of MPI are also inserted in Fig. 2(c). MPI noise causes fluctuations across the four PAM levels, with higher levels experiencing more severe distortion. This fluctuation can lead to the PAM levels crossing decision thresholds, resulting in incorrect symbol decision.

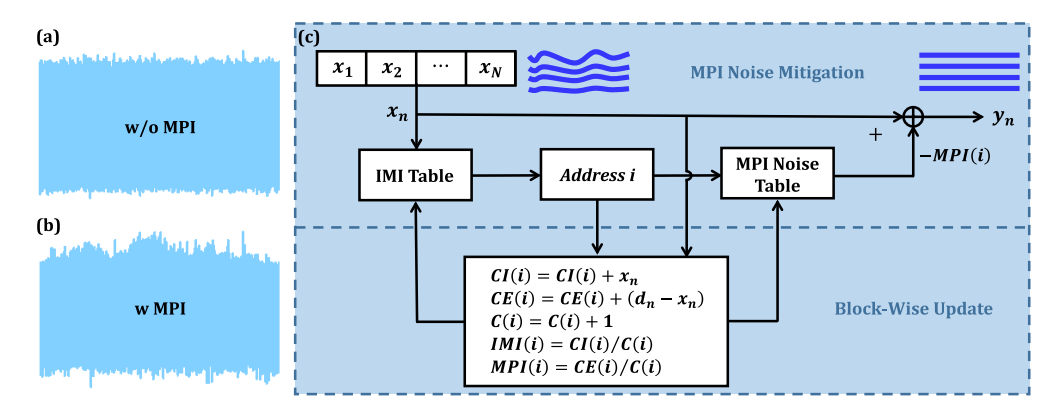


Fig. 2. PAM4 signal profiles (a) without MPI and (b) with MPI, and (c) the schematic diagram of the proposed IMIA scheme.

To eliminate the adverse effect of signal fluctuation, we propose an MPI noise mitigation scheme based on instantaneous mean intensity addressing (IMIA), as shown in Fig. 2(c). Before the processing of IMIA scheme, the received signal is segmented into data block. The proposed IMIA scheme operates in two primary phases, i.e., MPI noise mitigation and block-wise update. In the part of MPI noise mitigation, an address i for the received signal x_n in the data block will be identified by referencing the pre-established IMI table. The IMI table stores the instantaneous mean intensity values for each PAM4 level. By comparing the actual received signal intensity with the values in the IMI table, an address is assigned to the received signal for MPI noise table addressing

$$i = \underset{i \in [1, 2, 3, 4]}{argmin} |IMI(i) - x_n|$$
(7)

The address i is then used to look up the MPI noise table, which stores the MPI distortion specific to each PAM level, to retrieve the MPI noise MPI(i) for the current signal. The corrected

signal y_n is obtained by subtracting the identified MPI noise from the received signal

$$y_n = x_n - MPI(i) \tag{8}$$

The purpose of the block-wise update part is to update the IMI table and MPI noise table periodically by processing a block of received symbols. Instead of updating the IMI and MPI noise tables after every individual symbol, the IMIA scheme processes symbols in block which typically contains a predefined number of symbols. In each block, the cumulative intensity *CI* and cumulative error *CE* are calculated to accumulate the total intensity and error sum for each PAM level respectively

$$CI(i) = CI(i) + x_n (9)$$

$$CE(i) = CE(i) + (d_n - x_n)$$
(10)

where d_n is the decision value of x_n , which is determined by the address i. A counter C records the number of updates applied for each PAM level within the block

$$C(i) = C(i) + 1 \tag{11}$$

After processing all symbols in the block, the IMIA scheme updates the IMI and MPI noise values for each PAM level in their respective tables by averaging the cumulative intensity CI and cumulative error CE

$$IMI(i) = CI(i)/C(i)$$
(12)

$$MPI(i) = CE(i)/C(i)$$
 (13)

The IMI and MPI noise tables are updated at the end of each block, which are used for the process of the upcoming block of symbols. With block-wise update, the IMIA scheme can adapt to the varying MPI noise levels in real-time, ensuring more accurate extraction of MPI noise.

4. Simulation setup

To evaluate the performance of the proposed IMIA scheme, a simulation of a 50-Gbps PAM4based optical transmission system was conducted using VPI Transmission Maker 11.3, followed by offline processing in MATLAB, as illustrated in Fig. 3. At the transmitter (Tx) side, a pseudorandom binary sequence (PRBS) is first converted into PAM4 symbols. These symbols are then shaped using a root-raised-cosine (RRC) filter with a roll-off factor of 0.1, upsampled to 4 samples per symbol (SPS), and transmitted through the VPI simulation environment. For the VPI transmission part, the 50-Gbps PAM4 signal is sent to a Mach-Zehnder modulator (MZM) with 3-dB bandwidth of 10 GHz. A continuous wave (CW) laser with wavelength of 1550 nm is used as and the launched optical power (LOP) is set to 10 dBm. The detailed simulation parameters are shown in Table 1. To simulate the MPI effects, two scenarios were tested: one with a single FTRL and another with four FTRLs. The optical signal was split into two or five paths after passing through a 10-km standard single-mode fiber (SSMF). In both scenarios, one path directly delivered the signal to the receiver, while the other paths (representing FTRLs) were routed through additional SSMF segments of different lengths. These additional paths introduced different delay times, simulating real MPI effect. Variable optical attenuators (VOA) were used to adjust both the MPI noise intensity and the received optical power (ROP) at the receiver. The transmitted signal and the FTRLs are coupled together and detected by a PIN. At the receiver (Rx), the signal was initially processed through a matched filter, followed by equalization using a feed-forward equalizer (FFE) with 21 taps. A training sequence with 2000 symbols is used to train the taps of FFE and initialize the IMI table and MPI noise table for the IMIA scheme. After equalization, the signal was downsampled to 1 SPS and processed using the IMIA scheme to mitigate MPI noise. Finally, the PAM4 symbols were demapped to calculate the bit error rate (BER).

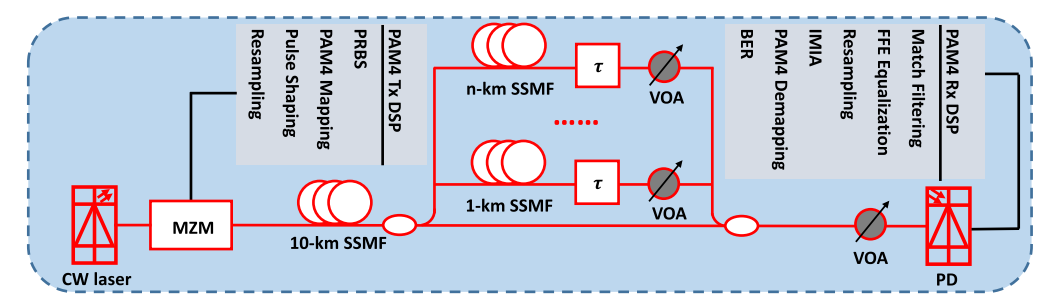


Fig. 3. Simulation setup for a 50-Gbps optical PAM4 IM/DD transmission system with

Table 1. Simulation parameters	
Parameters	Values
Data Rate	50 Gbps
Laser wavelength	1550 nm
Laser linewidth	100 kHz/1 MHz/ 5 MHz
LOP	10 dBm
MZM bandwidth	$10\mathrm{GHz}$
Transmission distance	10 km
ROP	-14.5 dBm

Results and discussion

The performance of the proposed IMIA scheme was initially evaluated within the 50-Gbps PAM4 optical transmission system with a single FTRL. In this setup, MPI was represented by the attenuation value of the VOA placed in the FTRL path, simulating the return loss from reflection points. We initially optimized the block size of the proposed IMIA scheme for different laser linewidths of 100 kHz, 1 MHz and 5 MHz, and the results are shown in Fig. 4. The optimal block sizes are 75, 30, and 15 symbols for laser linewidths of 100 kHz, 1 MHz and 5 MHz, respectively. For narrower linewidths, such as 100 kHz, the MPI noise exhibits less fluctuation, allowing larger block sizes to effectively capture and mitigate the MPI noise. Conversely, broader linewidths, such as 5 MHz, introduce more rapid signal fluctuation, requiring smaller block size to accurately track the dynamic noise.

The BER performance of the 50-Gbps PAM4 signal was analyzed across a range of MPI levels, as illustrated in Fig. 5. For a more comprehensive evaluation, the performance of the IMIA scheme is compared with two other schemes, the cascade of A1 and A2 (A1@A2) and the ADT scheme. The parameters of A1@A2 algorithm to be optimized are the symbol lengths N_1 and N_2 for A1 and A2 algorithms, which are optimized when the MPI level is -16 dB, and the optimized results are (2700, 160), (1000, 50) and (1900, 30) when the laser linewidths are 100 kHz, 1 MHz and 5 MHz respectively. The A1@A2 scheme demonstrates significant improvement in BER performance under various laser linewidths. The IMIA scheme achieves comparable performance to the ADT scheme and demonstrates better BER results than the A1@A2 scheme. The A1@A2 scheme estimates a single MPI noise value and applies it to all PAM4 levels with varying weights. In contrast, the IMIA scheme uses IMI and MPI noise tables to extract specific MPI noise values for each PAM4 level, which addresses the amplitude-dependent characteristics of MPI noise, allowing for more precise MPI noise mitigation. However, performance gaps between the IMIA and ADT can be observed when the MPI is low. When the MPI level is low, the distortions introduced by MPI are less significant, resulting in only minor deviations from the expected signal

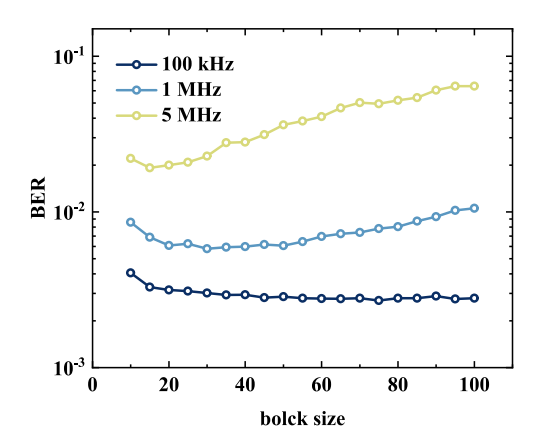


Fig. 4. Block size optimization under the MPI of -16 dB.

intensities. In such cases, the MPI noise removal process of the IMIA scheme may lead to slight overcompensation, leading to the observed performance gap. Considering two forward error correction (FEC) thresholds, i.e., the 7% HD-FEC (3.8×10^{-3}) and the KP4-FEC (2.4×10^{-4}), the IMIA scheme exhibits outstanding MPI tolerance across different transmission conditions. Under the 7% HD-FEC criterion, the IMIA scheme achieves MPI tolerances of 8 dB, 8 dB, and 6 dB for laser linewidths of 100 kHz, 1 MHz, and 5 MHz, respectively. For the KP4-FEC criterion, the IMIA scheme shows tolerance improvements of 6 dB, 4 dB, and 4 dB under the same respective linewidths. These results highlight the effectiveness of the proposed IMIA scheme in maintaining robust MPI tolerance across different MPI levels and laser linewidths.

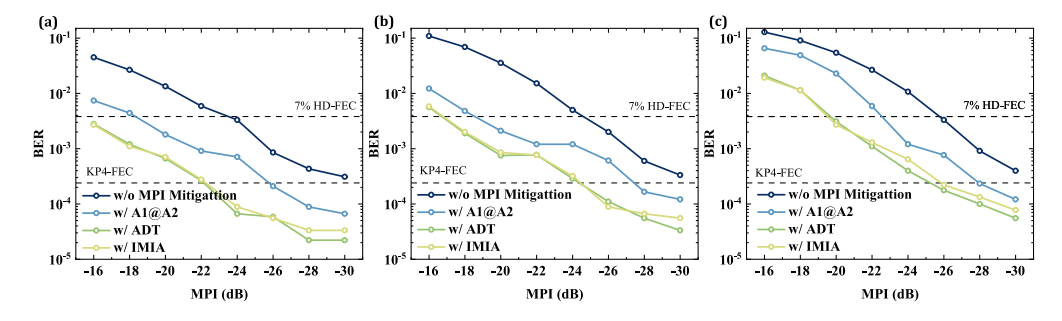


Fig. 5. BER performance versus MPI levels under different laser linewidths: (a) 100 kHz, (b) 1 MHz, and (c) 5 MHz.

Figure 6(a) 6(c) shows the received PAM4 levels without MPI mitigation, and with the compensations of A1@A2 scheme and the proposed IMIA scheme. The laser linewidth was set to 100 kHz, and the MPI level was set to 20 dB. Without any MPI mitigation, the received PAM levels display irregular instantaneous intensity fluctuations, with higher PAM levels experiencing more severe fluctuations, which greatly degrades the performance of the system with a BER value of 1.3×10^{-2} . When applying the A1@A2 scheme to suppress the MPI noise, the instantaneous intensity fluctuations can be mitigated, the BER is reduced by an order of magnitude to 1.8×10^{-3} . However, there are still slight residual fluctuations in the PAM levels. In contrast, with the proposed IMIA scheme, the instantaneous intensity fluctuations are nearly eliminated, demonstrating the high effectiveness of the IMIA scheme in mitigating MPI noise. This further reduces the BER by another order of magnitude to 7.1×10^{-4} .

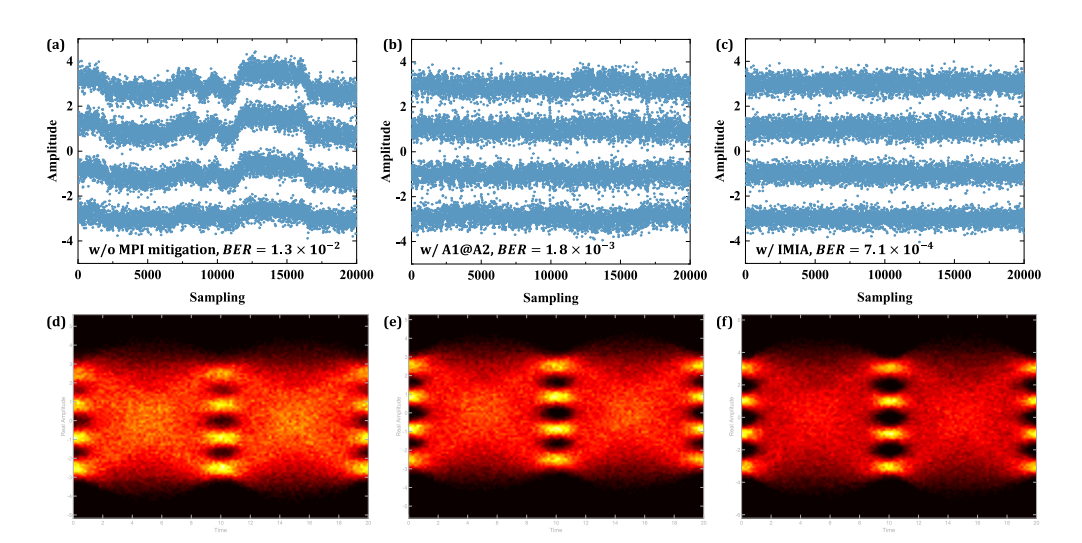


Fig. 6. The PAM4 signal levels (a) without MPI mitigation (BER = 1.3×10^{-2}), (b) with the A1@A2 scheme (BER = 1.8×10^{-3}), and (c) with the IMIA scheme (BER = 7.1×10^{-4}), along with their corresponding eye diagrams (d)-(f).

The corresponding eye diagrams, as shown in Fig. 6(d) 6(f), also illustrate the impact of MPI noise and the improvements achieved by the A1@A2 and IMIA schemes. MPI noise causes noticeable closure in the eye openings and this closure is especially severe at higher PAM levels. When the A1@A2 scheme is applied, as shown in Fig. 6(e), the eye openings are improved compared to the unmitigated case, with clearer level separations and reduced noise interference. In Fig. 6(f), the IMIA scheme further optimizes the eye diagram. The IMIA scheme effectively eliminates most MPI noise, resulting in wide, clear and well-defined eye openings.

The iteration curves for IMI and MPI noise during the block-wise updating process under a laser linewidth of 100 kHz and an MPI level of 20 dB are shown in Fig. 7. Figure 7(a) shows the IMI values for each PAM4 level, which dynamically track signal fluctuations during the updating process, providing accurate references for the current received signal. In Fig. 7(b), the extracted MPI noise for each PAM4 level precisely captures the amplitude-dependent nature of MPI noise. These curves illustrate how the IMIA scheme effectively tracks and compensates for varying noise levels in real-time.

By integrating with NWF and MLSE, the performance of the A1@A2 and IMIA schemes can be further enhanced, as depicted in Fig. 8. Specifically, for the laser linewidths of 100 kHz and 1 MHz, this integration enables the IMIA scheme to achieve an extra 2-dB improvement in MPI tolerance when satisfying the KP4-FEC criterion. This result indicates that, with the NWF and MLSE processing, the IMIA scheme enables the system to tolerate stronger MPI noise levels than the ADT scheme. For the laser linewidth of 5 MHz, while this integration does not yield measurable increase in MPI tolerance in terms of decibels, a significant reduction in BER can still be observed. Therefore, integrating the NWF and MLSE with the IMIA scheme can improve the system performance across varying laser linewidths, with particularly additional gains in MPI tolerance for low linewidths and significant BER reduction for high linewidths, demonstrating the effectiveness of these combined approaches.

In the above simulations, a VOA was placed at the receiver side to adjust the ROPs, which was set to -14.5 dBm across all simulations. The BER performance of different mitigation schemes was then compared at varying ROPs, as shown in Fig. 9. For this test, the laser linewidth and the MPI level were fixed at 100 kHz and -24 dB, respectively. Without MPI noise, the system

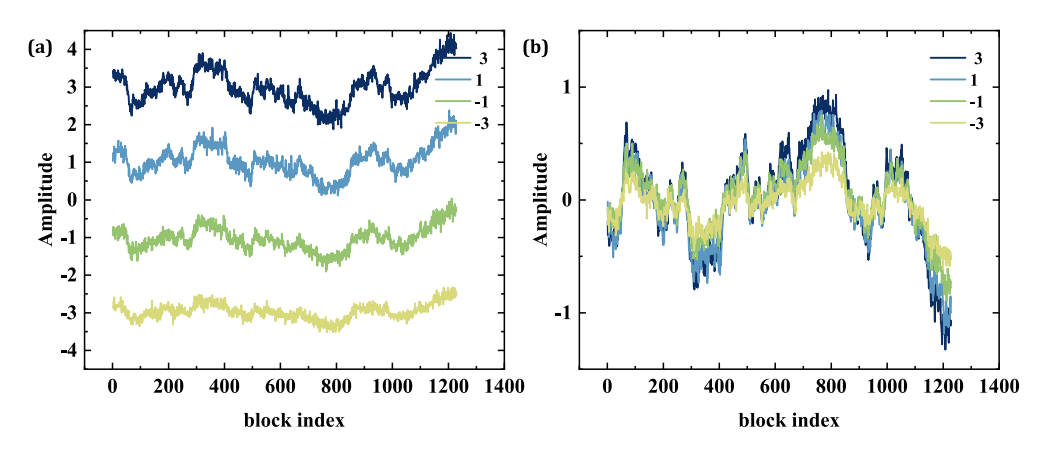


Fig. 7. The iteration curves for (a) IMI and (b) MPI noise during the block-wise updating process.

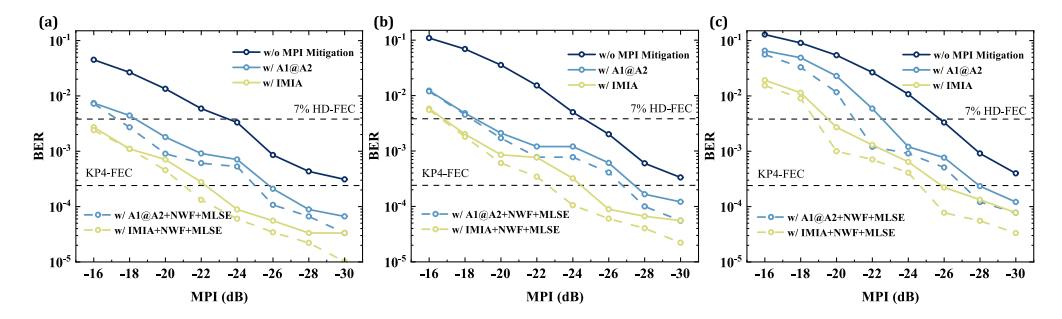


Fig. 8. BER performance versus MPI levels under different laser linewidths: (a) 100 kHz, (b) 1 MHz and (c) 5 MHz.

requires a ROP of -17 dBm to meet the 7% HD-FEC threshold and -15.5 dBm to meet the KP4-FEC threshold. However, when MPI noise is present, BER performance is significantly impaired, with the system requiring a ROP of -14.5 dBm to meet the 7% HD-FEC threshold, but unable to satisfy the KP4-FEC threshold. With the A1@A2 scheme, the receiver sensitivity is improved by 1.5 dB, and the system requires -16 dBm of ROP to meet the 7% HD-FEC criterion while still fails to satisfy the KP4-FEC criterion. In contrast, both the IMIA and ADT schemes improve receiver sensitivity by an additional 1 dB, allowing the system to meet the 7% HD-FEC criterion at a ROP of -17 dBm. These two schemes also enable the system to satisfy the KP4-FEC criteria at the ROP of -15 dBm. Moreover, when the A1@A2 scheme is integrated with NWF and MLSE, the system successfully reduces the BER below the KP4-FEC threshold with an ROP of -14.5 dBm. Additionally, when combined with NWF and MLSE, the IMIA scheme achieves performance comparable to the no-MPI case across different ROPs.

In previous simulations, we focused on the impact of a single FTRL on system performance. However, in practical applications, MPI typically results from the cumulative interference of multiple FTRLs. To further evaluate the effectiveness of the proposed IMIA scheme, we extended our simulation to a 50-Gbps PAM4 transmission system influenced by four distinct FTRLs. Each of these FTRLs traveled through additional SSMF lengths of 1 km, 2 km, 3 km, and 4 km, respectively, introducing unique delays corresponding to their fiber lengths. The laser linewidth was set to 100 kHz for this simulation.

The results, as shown in Fig. 10, demonstrate the robustness of the IMIA scheme in MPI scenario involving multiple FTRLs. We can observe in Fig. 10(a) that the IMIA scheme performs

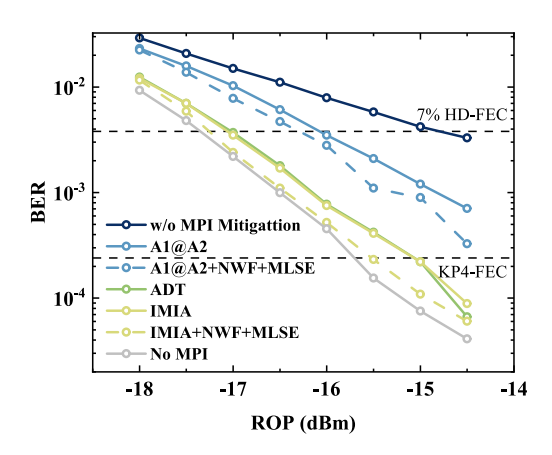


Fig. 9. BER performance versus ROPs under 100-kHz laser linewidth and -24-dB MPI level.

similarly to the single-FTRL case, having comparable performance to the ADT scheme and outperforming the A1@A2 scheme. For this multi-FTRL scenario, the IMIA scheme achieves MPI tolerances of 6 dB for the 7% HD-FEC criterion and more than 4 dB for the KP4-FEC criterion. In addition, the NWF and MLSE were employed to further enhance the performance of the A1@A2 and IMIA schemes, as shown in Fig. 10(b). With the integration of NWF and MLSE, the BER for both schemes is significantly reduced, achieving an additional 2-dB improvement in MPI tolerance under the KP4-FEC criterion.

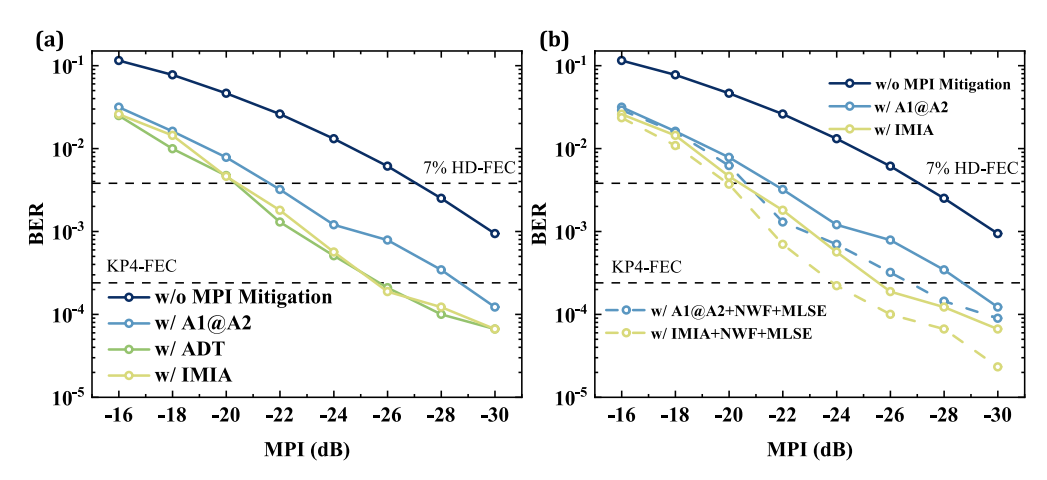


Fig. 10. BER performance versus MPI with four FTRLs under 100-kHz laser linewidth (a) without NWF and MLSE, and (b) with NWF and MLSE.

The A1@A2 scheme processes each received symbol individually. For every symbol, hundreds or even thousands of addition operations and a few multiplication operations are required, resulting in high computational cost. In contrast, both the IMIA and ADT schemes operate on a block-wise basis, typically processing blocks containing tens of symbols. Each block requires only one update of IMI and MPI noise tables (for IMIA) or decision thresholds (for ADT). As a result, the operations required for IMIA and ADT per symbol are negligible compared to the A1@A2 scheme. Therefore, the IMIA and ADT schemes offer significantly lower complexity than the A1@A2 scheme due to their block-wise processing approach.

6. Conclusion

In this paper, we have proposed an MPI noise mitigation scheme IMIA to enhance the MPI tolerance in PAM4-based IM/DD systems. The IMIA scheme mitigates MPI noise through real-time referencing of an IMI table and an MPI noise table, and the block-wise updating mechanism for these tables allows the IMIA scheme to dynamically track and adapt to changes in MPI noise over time. Simulations in a 50-Gbps PAM4 transmission system demonstrated the robustness of the IMIA scheme across varying MPI levels and laser linewidths. Through simulations in a 50-Gbps PAM4 transmission system, the IMIA scheme demonstrated robust performance across various MPI levels and laser linewidths. The results indicate that the IMIA scheme achieves similar performance to our previously proposed ADT scheme, providing MPI tolerances exceeding 6 dB and 4 dB for the 7% HD-FEC and KP4-FEC thresholds, respectively. Additionally, the IMIA scheme has compatibility with other advanced algorithms. By integrating with NWF and MLSE, the IMIA scheme can obtain extra MPI tolerance gains of 2 dB. The IMIA scheme thus offers a highly effective solution for MPI mitigation, with considerable potential for deployment in high-density, short-reach optical networks.

Funding. Hong Kong Research Grants Council (GRF15209321).

Disclosures. The authors declare no conflicts of interest.

Data availability. Data underlying the results presented in this paper are not publicly available at this time but may be obtained from the authors upon reasonable request.

References

- S. M. Ranzini, R. Dischler, F. Da Ros, et al., "Experimental investigation of optoelectronic receiver with reservoir computing in short reach optical fiber communications," J. Lightwave Technol. 39(8), 2460–2467 (2021).
- K. Zhong, X. Zhou, J. Huo, et al., "Digital signal processing for short-reach optical communications: A review of current technologies and future trends," J. Lightwave Technol. 36(2), 377–400 (2018).
- A. Chaaban, Z. Rezki, and M.-S. Alouini, "On the capacity of intensity-modulation direct-detection Gaussian optical wireless communication channels: A tutorial," IEEE Commun. Surv. Tutorials 24(1), 455–491 (2022).
- J. Cheng, C. Xie, Y. Chen, et al., "Comparison of coherent and IMDD transceivers for intra datacenter optical interconnects," in Optical Fiber Communications Conference (2019), pp. 1–3.
- 5. M. Chagnon, "Optical communications for short reach," J. Lightwave Technol. 37(8), 1779-1797 (2019).
- K. Zhong, X. Zhou, T. Gui, et al., "Experimental study of PAM-4, CAP-16, and DMT for 100 Gb/s short reach optical transmission systems," Opt. Express 23(2), 1176–1189 (2015).
- 7. E. Maniloff, S. Gareau, and M. Moyer, "400 G and beyond: Coherent evolution to high-capacity inter data center links," in *Optical Fiber Communications Conference* (2019), pp. 1–3.
- T. Chen, X. Gao, and G. Chen, "The features, hardware, and architectures of data center networks: A survey," J. Parallel Distr. Com. 96, 45–74 (2016).
- J. L. Gimlett and N. K. Cheung, "Effects of phase-to-intensity noise conversion by multiple reflections on gigabit-persecond DFB laser transmission systems," J. Lightwave Technol. 7(6), 888–895 (1989).
- D. A. Fishman, D. G. Duff, and J. A. Nagel, "Measurements and simulation of multipath interference for 1.7-Gb/s lightwave transmission systems using single-and multifrequency lasers," J. Lightwave Technol. 8(6), 894–905 (1990).
- 11. C. R. S. Fludger, M. Mazzini, T. Kupfer, et al., "Experimental measurements of the impact of multi-path interference on PAM signals," In in Optical Fiber Communications Conference (2014), pp. 1–3.
- 12. Y. J. Wen, Y. Cui, and Y. Bai, "Mitigation of optical multipath interference impact for directly detected PAMn system," Opt. Express 28(25), 38317–38333 (2020).
- C. Huang, H. Song, L. Dai, et al., "Optical multipath interference mitigation for high-speed PAM4 IMDD transmission system," J. Lightwave Technol. 40(16), 5490–5501 (2022).
- K. Lian, J. Liu, D. Wang, et al., "Balanced coding schemes for optical multipath interference suppression in pam4-imdd systems," in Asia Communications and Photonics Conference (2022), pp. 698–701.
- A. Ulhassan, T. Pham, Q. Wang, et al., "Statistical method for multi-path interference detection in IMDD optical links," J. Lightwave Technol. 41(14), 4699–4704 (2023).
- Y. Li, Z. Wei, B. Deng, et al., "Adaptive decision threshold for an optical multipath-interference-impaired short-reach 50-Gbps PAM4 transmission," Opt. Lett. 48(21), 5675–5678 (2023).
- 17. W. R. Peng, Y. Zhu, C. Samina, et al., "Adaptive noise whitening filter and its use with maximum likelihood sequence estimation," in *Optical Fiber Communication Conference* (2016), paper Tu3K-7.